Analytical Methods

Accepted Manuscript

This is an *Accepted Manuscript*, which has been through the RSC Publishing peer review process and has been accepted for publication.

Accepted Manuscripts are published online shortly after acceptance, which is prior to technical editing, formatting and proof reading. This free service from RSC Publishing allows authors to make their results available to the community, in citable form, before publication of the edited article. This *Accepted Manuscript* will be replaced by the edited and formatted *Advance Article* as soon as this is available.

To cite this manuscript please use its permanent Digital Object Identifier (DOI®), which is identical for all formats of publication.

More information about *Accepted Manuscripts* can be found in the **Information for Authors**.

Please note that technical editing may introduce minor changes to the text and/or graphics contained in the manuscript submitted by the author(s) which may alter content, and that the standard **Terms & Conditions** and the **ethical guidelines** that apply to the journal are still applicable. In no event shall the RSC be held responsible for any errors or omissions in these *Accepted Manuscript* manuscripts or any consequences arising from the use of any information contained in them.

CHARACTERIZATION OF DUAL BIOTIN TAG FOR IMPROVED SINGLE STRANDED DNA PRODUCTION

Meral Yuce[1*], Hasan Kurt[2], Hikmet Budak[1,2]

[1*] Sabanci University, Nanotechnology Research and Application Centre, 34956, Istanbul, Turkey

[2] Sabanci University, Faculty of Engineering and Natural Sciences, 34956, Istanbul, Turkey

*** Corresponding author phone: + (90) 536 382 6105**

Email address: meralyuce@sabanciuniv.edu

ABSTRACT

Generation of single-stranded DNA plays a key role in many biotechnology applications including production of aptamers, single strand conformation polymorphism, nuclease S1 mapping, pyrosequencing, genosensors, probe preparation and labelling, subtractive hybridization as well as nucleic acid sensing and microarrays. Several methods are available in the literature to produce single-stranded DNA from double-stranded DNA template, such as extraction of the sense strand from denaturing gels, asymmetric PCR, use of streptavidin-biotin interaction, and some alternative methods, including enzymatic digestion of negative strand by either Lambda exonuclease or T7 Gene 6 exonuclease. In this report, a detailed characterization of dual biotin tag method to generate single-stranded DNA from the random oligonucleotide library is presented. Unlike the traditional streptavidin-biotin method that uses single biotin tagged molecule during separation, this novel technique is based on a dual biotin molecule covalently attached to 5' end of the negative strand. Improved technique takes less than one hour as a consequence of eliminated alkali treatment step, which make this procedure the shortest procedure described in literature so far for single-stranded DNA production. The method can achieve a single-stranded DNA yield around 75% from the corresponding DNA template in Tris-HCl buffer. A number of parameters, such as the effect of different elution buffers and heat treatments, spontaneous release of streptavidin from the magnetic bead surface, loss of beads during consecutive washes, aggregation of the beads, were investigated to reveal the optimal conditions for single-stranded DNA production. FTIR, DLS, SEM, and Electrophoresis techniques were used for characterization studies.

Keywords: Dual Biotin, single-stranded DNA, Aptamer, Oligonucleotide, Magnetic beads

1. Introduction

There are several methods available in the literature for single-stranded DNA (ssDNA) production from the corresponding double-stranded DNA (dsDNA) template. These methods include asymmetric PCR[1,2] biotin–streptavidin separation via magnetic beads[3,4] digestion of antisense strand[5] and size dependent separation on denaturing urea polyacrylamide gel electrophoresis (PAGE).[6–8] The purity and yield of ssDNA outline the success of each application. Generation of ssDNA is generally time-consuming and expensive process since numerous purification steps are involved. Not only the purification is a time intensive and expensive process, but also it results in significant loss of ssDNA around 30%. Additionally, last pool should be liberated from any reaction impurities, such as remaining dsDNA as well as proteins. Urea PAGE is one of those conventional methods that induces traceable migration of two strands of DNA on the gel and allows selective excision of any of the strands.[9] Urea breaks the hydrogen bonds between the strands of the amplicon as the DNA melting temperature is lowered and causes differential migration of the strands in the gel.[10] In this case, the sense strand has to be extracted and purified, which makes the process cumbersome and time-consuming, even though it can potentially produce high purity ssDNA. In addition, these purification steps results in significantly low yields of ssDNA, which renders the process unappealing. Another widely used method is asymmetric PCR which produces ssDNA through unequal amounts of sense and antisense primers used in the PCR.[11] There are two main steps of amplification in the asymmetric PCR. The first phase, which proceeds exponentially, is to produce enough amount of dsDNA as starting material. The next phase is the linear amplification phase that produces the actual ssDNA. Asymmetric PCR is commonly unidirectional, relying on either the forward or reverse primer or dependent on the presence of both primers of different concentrations, by use of dsDNA as the template. Although the asymmetric PCR method has become prevalent in the ssDNA production due to being cost effective, it still needs reaction optimization for each sample, and more importantly, the final product has to be purified to clean out any reaction residue or dsDNA used as a template. Recently, use of digestive enzymes for the ssDNA production has been become popular. It has been reported that a fast and efficient method for the ssDNA production with high quality and yield relying on lambda exonuclease digestion was utilized.[5] Lambda exonuclease originating from bacteriophage l, is an enzyme that involved in the repair of double-stranded breaks of the viral DNA. It selectively digests the phosphorylated strand(s) of double-stranded DNA from the 5' to the 3' end, because of its strong affinity for a phosphorylated 5'end rather than a hydroxylated 5'end.[12] During the ssDNA production via lambda exonuclease, a 5' phosphate group, is introduced into one strand of dsDNA by performing PCR where only one of the two primers is 5' phosphorylated.[13] PCR reaction is treated with lambda exonuclease under optimal conditions and phosphorylated strand is removed by enzymatic digestion while non-phosphorylated strand stays in the mixture.[14,15] Although lambda

exonuclease digestion is efficient in terms of yield, the high cost of the enzyme, requirement for additional purification step to get rid of the digested elements, and incomplete digestion of the phosphorylated PCR product[16], which could lead to the accumulation of the dsDNA in the reaction mixture, makes the process unfavourable. In the traditional method of biotin–streptavidin separation, one of the primers is biotinylated and the resulting biotinylated PCR product is immobilized onto the streptavidin-coated surfaces.[17,18] Due to the high affinity[19] of the streptavidin towards the biotin, with a dissociation constant (K_d) in the order of $4x10^{-14}$ M , the desired non-biotinylated strand is separated from the biotinylated strand by alkaline treatment (NaOH) and subsequently concentrated by ethanol precipitation. The smart-PCR system was also reported as a combination of asymmetric PCR and biotin–streptavidin separation.[20] The asymmetric PCR product containing biotin at one end was loaded onto the streptavidin-immobilized column. Following the washing step to remove excess dNTPs, primers and other PCR components, ssDNA was eluted from the column by alkaline treatment. The ease of removing the non-biotinylated strand from biotinylated strands with NaOH is responsible for the wide use of biotin–streptavidin separation to generate ssDNA in a number of DNA aptamer studies. Although the biotin–streptavidin interaction is very much favoured for DNA strand separation, there are still some problems such as contamination of the final pool with either biotinylated negative strand or streptavidin. For example, during aptamer production, these negative biotinylated strands could reanneal with the complementary strand and reduce the structural properties, which is essential for target binding. On the other hand, release of the streptavidin from the surface of magnetic beads creates a second target molecule within the final pool due to its RGD (Arg-Gly-Asp) motif mimicking RYD sequence (Arg-Tyr-Asp)[21], which leads production of non-specific oligonucleotides. These are all due to alkali treatment that disturbs not only hydrogen bonds between the bases but also bonds between biotin-streptavidin and streptavidin-magnetic bead. As a result, either biotinylated strand or streptavidin leak into final solution and creates a significant problem for applications like SELEX.[3] A summary of ssDNA production techniques is presented in Supplementary Data [Table 1].

In this report, utilization of the dual biotin tag in ssDNA production was explored for the first time. A schematic explanation of the method is given on Scheme 1. A dual biotin molecule attached in one sequence (negative strand) can strengthen binding ability of the strand towards streptavidin, which keeps biotinylated DNA strand more stable on the surface of streptavidin-coated material for downstream applications.[22,23] Dual biotin tag has been previously addressed in SAGE[24] (Serial Analysis of Gene Expression) and DNA sequencing studies[25,26], where the dual biotinylated primer attached on the streptavidin beads allowed direct sequencing of amplified DNA. Adoption of dual biotinylated oligonucleotides into quantum dot based nanostructures was also reported.[27] However, a detailed characterization and optimization of dual biotin tag for the ssDNA production has not been disclosed previously. In the presented report, employment of dual biotin tag during ssDNA production

was assessed under different experimental conditions. Research was designed to inspect possible risks lowering the final ssDNA yield, such as selection of elution buffer, heat treatment, incubation time, agglomeration of the streptavidin-coated beads, loss of beads during consecutive washes and protein contamination. Upgraded method requires a couple of PCR rounds followed by incubation with the beads, and it provides elution of the ssDNA in a simple way that eliminates alkaline treatment, or purification steps.

<Here Scheme 1>

2. Experimental

2.1. Chemicals

Streptavidin-coated magnetic beads were purchased from Invitrogen (MyOne C1, Life Technologies Corporation, CA, USA). 94mer synthetic oligonucleotide (O_{94}) and the primers were purchased from Microsynth (Switzerland). 94mer oligonucleotide had 49-nucleotide random sequence flanked with primer binding sites at both ends (5' AGCTCCAGAAGATAAATTACAGG [N49] CA ACTAGGATACTATGACCCC 3'). Single-stranded short oligonucleotide (O_{23}), which was further used as forward primer, had a dual biotin tag at 5'end (5' Bio/AGCTCCAGAAGATAAATTAC AGG 3') and reverse primer was free of label (5' GGGGTCATAGTATCCTAGTTG 3'). According to information provided by the manufacturer, one of the biotin molecules is introduced via 5'end modification while the other biotin is an internal modification on the subsequent dNTP. Chemical structure diagram of the dual biotin molecule was drawn by Accelrys Draw v4.0, and presented in Scheme 1. All glassware and solutions were autoclaved in advance with HMC (Hirayama autoclave, Che Scientific Co., Hong Kong).

Elution solutions were TBE (Tris Borate EDTA; 89 mM Tris base, 89 mM Boric acid, 2 mM EDTA, pH 8.0), PBS (Phosphate Buffered Saline; 137 mM NaCl (Riedel de Haen), 2.7 mM KCl, 4.3 mM Na_2HPO_4-$7H_2O$, 1.4 mM KH_2PO_4, pH 7.4), Tris-HCl (10 mM Tris-HCl, pH 8.5, Elution Buffer or EB from QIAGEN), SSC (Saline sodium citrate; 15 mM $C_6H_5Na_3O_7$-$2H_2O$, 150 mM NaCl, pH 7.0), NaCl (Sodium chloride, 150 mM), NaOH (Sodium hydroxide, 150 mM), B&W buffer (Binding and wash buffer; 10 mM Tris-HCl, 1 mM EDTA and 2 M NaCl, pH 7.5) and distilled sterile water (DSW). Unless otherwise stated, all chemicals were purchased from Merck, Germany. All experiments were performed three times unless otherwise stated.

2.2. PCR and DNA purification

O_{94} was amplified using KAPA2G Robust PCR Kit with dNTPs (KAPA Biosystems, MA, USA) by following the protocol: 50 µl reaction mixture contained 1U of KAPA2G Robust DNA Polymerase, 10 µl of KAPA2G Buffer A, 10 µl of KAPA2G Enhancer 1, 1 µl KAPA2G dNTP mix

(200 µM), 1 µl of $MgCl_2$ (25 mM), DNAase free water, and 25 pmol of each primer. Thermal protocol was optimized to be 3 min at 95 °C, followed by 7 cycles of 30 seconds at 95 °C, 30 seconds at 60 °C, and 30 seconds at 72 °C. A final extension step of 72 °C for 5 min was included in all protocols. Thermal cycling was performed in Master Cycler® Gradient 384 (Eppendorf, NY, USA). PCR product was purified with Min Elute PCR purification kit (QIAGEN) in order to clean dsDNA from primers, dNTPs, and salts, by the selective binding of dsDNA to silica based spin column in the presence of chaotropic salts. Purification was performed by following the manufacturer's procedure.

2.3. Agarose Gel Electrophoresis

Sample quality was analysed with electrophoresis on 2% agarose gel[28] (PeqGold, High Quality Agarose, DE, USA). Five µl of the PCR product was mixed with 2 µl of 6X gel loading buffer and ran at 135 V for 30 min, and stained with Ethidium bromide (10 mg/ml). In the case of ssDNA, 2 µl of NaOH (150 mM) was included in gel samples. The bands were visualized with a UV box, and processed by ImageJ software according to intensity in pixels.[29]

2.4. Incubation of oligonucleotides with streptavidin-coated magnetic beads

O_{94} was dual biotinylated during PCR via dual biotinylated forward primer, and the biotinylated amplicon was captured using the streptavidin-coated beads. In the first place, recommended concentration of the beads was transferred into Eppendorf tube and washed three times with B&W in order to remove any preservative. Between each washing step, Eppendorf tube was vortexed for 10 seconds, placed in contact with a magnet for 2 min, and the supernatant was discarded with a micropipette. The magnetic beads were subsequently re-suspended in B&W buffer and incubated with any of the following: dual biotinylated ssDNA (O_{23}), purified dual biotinylated PCR product (O_{94}) or non-purified dual biotinylated PCR product. The incubation time was optimized for the both O_{23} and O_{94} by sampling the mixture every 15 min over a period of 90 min. Following the immobilisation of the biotinylated oligonucleotides on the beads, the tube was placed in the magnet for 2 min. The beads recovered were washed six times with B&W buffer. Unless otherwise stated all experiments were performed with 75 µg of the beads, which is equal to 7.5 µl of the original bead stock. According to the manufacturer's information, 1 mg of the beads can bind around 20 µg dsDNA or 500 pmol of ssDNA depending on the size of the product.

2.5. Elution of ssDNA from streptavidin-coated magnetic beads

Elution of ssDNA, spontaneous release of dual biotinylated DNA and streptavidin from the bead surface were investigated at elevated temperatures (75, 85 and 95 ºC) in following buffers; TBE, PBS, Tris-HCl, SSC, NaCl, NaOH, B&W and DSW. For this purpose, 60 µl of the beads were collected from the stock, washed three times with B&W buffer and re-suspended in B&W buffer.

Then, 300 pmol of O_{23} (dual biotinylated ssDNA), which is the maximum concentration of single-stranded oligonucleotide that can be captured by the given number of the beads according to the manufacturer, was added to the solution and incubated at room temperature for 30 min. The beads recovered with a magnet were divided equally into eight Eppendorf tubes for the elution step (each tube includes 7.5 µg beads). After the wash step (6X with B&W), the supernatants were discarded via magnetic separator and any of the following elution solutions was transferred into individual tubes; TBE, PBS, Tris-HCl, SSC, NaCl, NaOH, B&W and DSW. Finally, all samples were briefly vortexed and heat-treated at75, 85 and 95 ºC for a period of 90 seconds. The supernatants collected from each tube after elution, were used to analyse the amount of O_{23} and/or streptavidin deployed spontaneously from the bead surface.

All optical measurements were performed at room temperature by using a Nanodrop Spectrophotometer (Nanodrop 2000c, Thermo scientific, USA). Nanodrop DNA-50 and DNA-33 applications provided within the equipment software, were used for quantification of dsDNA and ssDNA, respectively. The blank solutions were the same as the elution solutions described earlier. The ssDNA recovery (%) of the samples was calculated by dividing the ssDNA concentration by the initial dsDNA concentration. For protein quantification, Nanodrop protein application was used which reads the absorbance at 280 nm in combination with either the mass extinction coefficient or the molar extinction coefficient to calculate the concentration of the protein. The biotinylated strand contamination in O_{94} assays was theoretically calculated from the optical results presented in section 3.1, based on fact that O_{23} is the biotinylated primer for $O_{94,}$ and it would show similar behaviour under the same experimental conditions. The portion of the contamination (calculated as ~20% for Tris-HCl buffer) was theoretically subtracted from the eluted ssDNA, which is presented in Fig 5.

2.6. Bead characterization

Loss of beads during consecutive washes was determined by Casy TT device with 1:10000 dilutions (CASY Cell Counter and Analyzer, Roche, Germany). Hydrodynamic size of the beads was measured by Dynamic Light Scattering (DLS) technique[30] using a Malvern Zetasizer Nano ZS (Malvern Instruments, ZEN3600, UK), which was equipped with a 633 nm He-Ne laser and operated at an angle of 173° at 23±0.10 °C. For DLS measurements, samples were diluted with deionised sterile water by a thousand fold and adjusted to 1 ml. Data processing is performed by NNLS algorithm using 45 measurement cycles for each sample (n=3, each independent measurement comprised of 15 scans). Scanning Electron Microscopy (SEM) analysis was performed by using an LEO Supra 35VP Field Emission Scanning Electron Microscope. SEM samples were drop casted on a clean silicon wafer with a surface area of $1\times1cm^2$ and vacuum dried. Further characterization of the beads was performed using Fourier transform infrared spectroscopy (FTIR, Nicolet iS10) in the

region of 550-4000 cm^{-1} at a resolution of 0.5 cm^{-1} in ATR mode. FTIR samples were drop casted on clean glass slides for uniform deposition of the treated beads.

3. Results and Discussion

3.1. Effect of elution buffers and heat-treatment on O_{23} bearing beads

A number of different elution buffers were monitored at different temperatures in order to monitor their behaviour on O_{23}bearing streptavidin-coated magnetic beads, Even though streptavidin-biotin interaction is the strongest non-covalent bond in biological systems, it is quite susceptible to buffer conditions, pH, temperature and ligands acquired biotin.[31] It has been reported that streptavidin can be denatured and detach from the magnetic beads under adverse circumstances.[32] Figure 1 demonstrates the behaviour of different elution buffers on O_{23} bearing magnetic beads, which were exposed to heat treatment at 75, 85 and 95 ºC for 90 seconds. NaOH is a common solution used to break hydrogen bonds between DNA strands [33] in order to generate ssDNA. As it can be seen from the Figure 1 that NaOH affected both the biotin-streptavidin and the streptavidin-bead interaction at all temperatures tested, and released the O_{23} from the bead surface at the highest degree comparing with other solutions. It has to be noted that discharge of the streptavidin from the bead would end up with discharge of the biotinylated molecules that are already attached to the streptavidin. On the other hand, the biotinylated ligands could release from the bead surface regardless of streptavidin release, as a result of weak interaction or nonspecific binding.[34] In a similar study where a single biotin tag was employed, denaturation was performed either by the addition of 20 µl of 150 mM NaOH solution for 3 min or by heating at 95 ºC for 5 min in PBS (10 mM, pH 7.4).[35] It was reported that, with heat treatment, 10 times more streptavidin, streptavidin–biotinylated ssDNA or streptavidin–biotinylated dsDNA had leached from the magnetic bead surface as comparing with alkaline treatment. Because of both the complexity of the interactions and the 95 ºC being very harsh for any biological interaction, elution at this temperature could not achieve a pure ssDNA pool.

On the other hand, amount of the material released from the bead surface showed a reduction at lower temperatures, 85 and 75 ºC in Tris-HCl. The lowest streptavidin contamination was observed in DSW and Tris-HCl solutions, which provides favourable conditions to minimize protein contamination in final ssDNA pool. In a recent report that single biotin tagged ssDNA was employed, it was shown that streptavidin-biotin interaction can be reversibly broken up to 100% in non-ionic aqueous solutions at temperatures above 70 ºC. However, we showed that use of dual biotin tag can improve the interaction between streptavidin and biotin because of higher thermal stability, and reduce the number of molecules released from the bead surface. That could be a significant remark for especially SELEX applications where the target purity is essential to obtain the tightest binding sequences. To increase the stringency and purity during SELEX, a) streptavidin-coated beads can be used as “negative or counter SELEX target” ; b) a lower amount of the streptavidin-coated beads can

be applied to the ssDNA pool before incubation with the target, which would eliminate any biotinylated strand left in the pool.

<Here Fig. 1>

It is worth to note that bare streptavidin on the magnetic beads degrades around 80 ºC while streptavidin contacted with biotin is much more stable at elevated temperatures.[36,37] Thereby, temperature around 85 ºC would be optimal to separate the non-biotinylated DNA strand without damaging the structure of the streptavidin on the beads. At the same time, melting temperature of the biotin labelled strand should be taken into consideration. Because, not all of the four-streptavidin subunits are coupled to the bead surface covalently, typically only one or two, it becomes almost inevitable to avoid the streptavidin contamination in the final elution after heat treatment. Evidently, biotin and streptavidin release was close to zero at 75 ºC for the case of DSW and Tris-HCl. In this case, it could be possible to separate a non-biotinylated strand with a melting temperature close to 75 ºC. However, melting temperature of O_{94} was 79.9 ºC, so the ssDNA yield was reasonably low at 75 ºC, as it was expected from the theory.

For further assessment of the surface properties of streptavidin-coated magnetic beads, FTIR spectroscopy was performed. Naive streptavidin-coated beads presented three characteristic IR absorption peaks for streptavidin [Fig 2A]. Spectra had two significant absorption peaks at 1634 cm^{-1} and 1521 cm^{-1} which were amide I (-C=O stretch) and amide II (-C-N stretch) stretches of the protein, respectively.[38] Also C-O- stretch was seen at 1346 cm^{-1}. Because most of the characteristic IR absorption peaks of DNA coincide with proteins[39,40], a distinct absorption peak for O_{23} was not detected. FTIR data showed that heat treatment of O_{23} bearing beads at 85 ºC in NaOH disrupted the streptavidin on the surface of the magnetic beads, caused the streptavidin detachment and eventually contamination of the final elution, which was tracked with the descending intensity of the related absorption peaks. On the other hand, the beads that were eluted at the same temperature in Tris-HCl buffer conserved their characteristic surface properties almost at the same level with O_{23} bearing beads and naive beads. This result was in good agreement with streptavidin release data presented in Fig 1. FTIR data also confirmed that alkaline treatment step used in traditional bead-based ssDNA production methods could be excluded since it deteriorate the bead surface. Consequently, the beads can be directly eluted in Tris-HCl or DSW after incubation, which would tremendously shorten the time, cost and labour spent during the ssDNA production.

<Here Fig. 2>

3.2. Characterization of streptavidin-coated magnetic beads

During ssDNA production via magnetic beads, it is worth to consider the bead loss after consecutive washes upon incubation with a target molecule. Because the ssDNA yield is proportional to the number of magnetic beads used, the bead loss during washes of the beads should be avoided as much as possible. Therefore, loss of the beads per experiment was investigated by using a cell counter device. It was shown that ~25% of the beads were disappeared after nine consecutive washes [Fig 2B]. The number of washes was reduced to three (recommended by the supplier), in order to reduce the number of beads wasted, and the beads were analysed by SEM to visualize the result of different number of washes. It was concluded that reducing the number of washes created massive bead aggregates, and the salt used included in B&W (NaCl) covered the beads like a shell [Fig 3A and B]. As a result, excess of the salt tremendously limited the surface area of the beads and so the biotin binding sites. It is obvious that that kind of shell would complicate and minimize the separation of non-biotinylated strand from the surface. This could be one of the reasons that final ssDNA yield had been found quite low in previous studies where similar procedures were performed.[35,5] As a result, the beads were carefully washed six times after the incubation step, which was good enough to keep the beads separated and discard the excess amount of salt impurities [Fig 3C and 3D].

<Here Fig. 3>

3.3. Effect of incubation time on ssDNA production via streptavidin-coated magnetic beads

The binding capacity of the streptavidin-coated magnetic beads used in this study was investigated with O_{23} and O_{94}. PCR conditions were optimized in advance in order to obtain a fine amount of dsDNA with minimum artefacts. Briefly, initial template concentration and the number of thermal cycles were kept as low as possible to reduce the appearance of any nonspecific side product, which also reduced the time spent for PCR. The concentration of the dual biotin labelled primer was carefully optimised as 30 pmol/50 µl PCR reaction, in order to minimise the nonessential binding on the beads. After optimization of each PCR component, PCR products were run on an agarose gel and according to the results, seven cycles of PCR was found to be optimal for further studies [Fig 4A]. The PCR product obtained was cleaned up for only direct saturation analysis of the beads. The purification step was intentionally skipped for further experiments to avoid loss of DNA, and to keep the procedure as time and cost effective as possible. According to the results obtained, the bead surface was saturated in around 15min at room temperature for both O_{23} and O_{94} [Fig 4B]. It was also observed that the binding capacity of the beads was reduced almost by half for dsDNA incubation, unlike to the information stated in the manufacturer's manual. This could be due to both the dual biotin tag that occupies more than one subunit of the streptavidin and the length of the oligonucleotides. The randomized nature of the dsDNA library could be another explanation for that

kind of saturation, which could provoke sequence-specific or non-specific binding, rather than label specific binding.

On the other side, it was observed that excess of the DNA and the salts in the incubation media, formed multiple layers around the beads, which were monitored by the increased hydrodynamic size of the beads, screened with DLS measurements [Fig 4C]. As it can be followed from the figure, particle size of the beads was obviously greater than expected size (actual size 1000 nm), which was a noticeable discrepancy compared with results from SEM. The particle size measured by the DLS method is based on the magnetite radius, the hydrated polymer at the magnetite surface, and partly by the particle complex, which consists of the magnetic particle, the associated water, solvated ions, and counter ions on which some polymer is attached,[41,42] and that is why the beads could aggregate or form clusters to some extent. Therefore, DLS size measurement data was used as a tool for comparison of relative size upon incubation with O_{94}, not for actual sizing. In addition to hydrodynamic size increment of the beads presented in Fig 4C, Polydispersity Index (PdI) of the beads also showed an increasing trend with increased amounts of O_{94} [Supplementary Data, Table 2]. Especially for the beads incubated with the highest amount of O_{94} (75 µl), PdI was indicative for possible agglomeration. For further confirmation, magnetic beads were analysed by SEM in order to check possible agglomerations or clusters upon incubation with the excess amount of O_{94}. It was noted that the incubation with the increased amount of O_{94} formed bead clusters at different dimensions [Supplementary Data, Fig 1]. The reason why SEM images showed big particle aggregates that were not detected by DLS, could be explained by the solvent evaporation effect during sample preparation. Since the water has a considerable amount of surface tension energy, during its evaporation, the liquid-gas interface can carry particles in the liquid interior area. Eventually it would concentrate most of the particles into a limited space.[43,44] In this process, any DNA attached on the surface of the beads would lead further agglomeration of the particles due to entanglement of DNA strains on independent magnetic beads. Based on this information, it becomes important to consider the incubation time and product concentration/volume while using magnetic beads for the ssDNA production. Therefore, only a calculated amount of the PCR product should be incubated with the beads for optimal results.

<Here Fig. 4>

The effect of elution temperature on the final ssDNA yield was studied by using a constant amount of O_{94} (~2 µg). The beads incubated with corresponding PCR product were heat-eluted in Tris-HCl at three different temperatures for a period of 90 seconds, and finally, the supernatants recovered were analysed for ssDNA concentration. As it can be followed from Fig 5A (inset), ssDNA yield at 95 ºC was higher than the maximum theoretical concentration of ssDNA, which can be explained by the release of the non-biotinylated strand from the bead surface along with the biotinylated strand, as

dsDNA. Since the melting temperature of O_{94} library was 79.9 ºC, no traceable band was detected on the agarose gel after elution at 75 ºC and the amount of ssDNA was lower than the expected concentration. However, elution at 85 ºC presented a clear band on the agarose gel. That was because, the heat treatment at 85 ºC was below the degradation temperature of the conjugated streptavidin and it was additionally above the melting temperature of O_{94} library.

Finally, reproducibility of the procedure was tested by incubating the beads (75 µg) with non-purified PCR product (10 µL) for 15 min under gentle rotation. The beads recovered from magnetic separation were washed six times with B&W buffer, and eluted in 15 µL of Tris-HCl at 85 ºC. Minimum ssDNA recovery yield was calculated as 68.8% while the maximum recovery yield was 77.2% from the five independent experiments prepared under equal conditions [Fig 5B].

<Here Fig. 5>

4. Conclusion

The work presented here assessed the use of the dual biotin tag technique for single-stranded DNA production from random oligonucleotide library via streptavidin-coated magnetic beads. Whilst none of the techniques provides 100% generation of pure ssDNA, this improved method requires only a few steps, which all takes less than one hour and provides around 75% ssDNA from the corresponding dsDNA. Besides, it does not require alkali treatment step followed by purification, and ssDNA can be eluted directly in Tris-HCl. It is important to note that final ssDNA yield could vary from one sample to another depending on the incubation conditions and the size of the template. However, the dual biotin tag can be replaced with the single biotin tag for any application requiring higher thermal stability, and finally, the technique can be adapted with liquid handling systems for routine assays.

5. Acknowledgement

This study was supported by Sabanci University Nanotechnology Research and Application Centre (SUNUM). We would like to thank Dr Stuart James Lucas for expert technical assisting with the Casy TT Device.

References

1. U. B. Gyllensten and H. A. Erlich, *Proc. Natl. Acad. Sci. USA*, 1988, **85**, 7652–7656.
2. Z.-C. Liu, L.-J. Zhao, Y.-F. Zhang, H.-L. Shi, and Y. Xie, *Yao Xue Xue Bao*, 2012, **47**, 1605–11.
3. A. Paul, M. Avci-Adali, G. Ziemer, and H. P. Wendel, *Oligonucleotides*, 2009, **19**, 243–254.
4. S. H. Suh and L.-A. Jaykus, *J. Biotechnol.*, 2013, **167**, 454–61.
5. M. Avci-Adali, A. Paul, N. Wilhelm, G. Ziemer, and H. P. Wendel, *Molecules*, 2010, **15**, 1–11.
6. F. Flett and H. Interthal, *Methods Mol. Biol.*, 2013, **1054**, 173–85.
7. H. Summer, R. Grämer, and P. Dröge, *J. Vis. Exp.*, 2009.
8. R. C. Lo and V. M. Ugaz, *Electrophoresis*, 2006, **27**, 373–86.
9. N. C. Pagratis, *Nucleic Acids Res.*, 1996, **24**, 3645–6.
10. R. W. Floyd, M. P. Stone, and W. K. Joklik, *Anal. Biochem.*, 1974, **59**, 599–609.
11. B. Kaltenboeck, J. W. Spatafora, X. Zhang, K. G. Kousoulas, M. Blackwell, and J. Storz, *Biotechniques*, 1992, **12**, 164, 166, 168–71.
12. A. P. Null, J. C. Hannis, and D. C. Muddiman, *Analyst*, 2000, **125**, 619–26.
13. N. Ardjomandi, J. Niederlaender, W. K. Aicher, S. Reinert, E. Schweizer, H.-P. Wendel, and D. Alexander, *Nucleic Acid Ther.*, 2013, **23**, 44–61.
14. R. G. Higuchi and H. Ochman, *Nucleic Acids Res.*, 1989, **17**, 5865.
15. S. Takagi, M. Kimura, and M. Katsuki, *Biotechniques*, 1993, **14**, 218–21.
16. K. S. Sriprakash, N. Lundh, M.-O. Huh, and C. M. Radding, *J. Biol. Chem.*, 1975, **250**, 5438–5445.
17. M. Espelund, R. A. Stacy, and K. S. Jakobsen, *Nucleic Acids Res.*, 1990, **18**, 6157–8.
18. D. Shangguan, Y. Li, Z. Tang, Z. C. Cao, H. W. Chen, P. Mallikaratchy, K. Sefah, C. J. Yang, and W. Tan, *Proc. Natl. Acad. Sci. U. S. A.*, 2006, **103**, 11838–43.
19. N. M. Green, *Methods Enzymol.*, 1990, **184**, 51–67.
20. E. Kai, K. Sumikura, K. Ikebukuro, and I. Karube, *Biotechnol. Tech.*, 1998, **12**, 935–939.
21. R. Alon, E. A. Bayer, and M. Wilchek, *Biochem. Biophys. Res. Commun.*, 1990, **170**, 1236–41.

22. D. Dressman, H. Yan, G. Traverso, K. W. Kinzler, and B. Vogelstein, *Proc. Natl. Acad. Sci. U. S. A.*, 2003, **100**, 8817–22.

23. F. Diehl, M. Li, Y. He, K. W. Kinzler, B. Vogelstein, and D. Dressman, *Nat. Methods*, 2006, **3**, 551–9.

24. T. A. Milne, K. Zhao, and J. L. Hess, *Methods Mol. Biol.*, 2009, **538**, 409–23.

25. B. H. Bowman and S. R. Palumbi, *Methods Enzymol.*, 1993, **224**, 399–406.

26. J. A. Mosberg, M. J. Lajoie, and G. M. Church, *Genetics*, 2010, **186**, 791–9.

27. S. K. Dixit, N. L. Goicochea, M.-C. Daniel, A. Murali, L. Bronstein, M. De, B. Stein, V. M. Rotello, C. C. Kao, and B. Dragnea, *Nano Lett.*, 2006, **6**, 1993–9.

28. M. Svobodová, A. Pinto, P. Nadal, and C. K. O' Sullivan, *Anal. Bioanal. Chem.*, 2012, **404**, 835–42.

29. C. A. Schneider, W. S. Rasband, and K. W. Eliceiri, *Nat. Methods*, 2012, **9**, 671–5.

30. T. Zardán Gómez de la Torre, M. Strömberg, C. Russell, J. Göransson, M. Nilsson, P. Svedlindh, and M. Strømme, *J. Phys. Chem. B*, 2010, **114**, 3707–13.

31. C. E. Chivers, E. Crozat, C. Chu, V. T. Moy, D. J. Sherratt, and M. Howarth, *Nat. Methods*, 2010, **7**, 391–3.

32. D.-W. Lee, K. M. Park, M. Banerjee, S. H. Ha, T. Lee, K. Suh, S. Paul, H. Jung, J. Kim, N. Selvapalam, S. H. Ryu, and K. Kim, *Nat. Chem.*, 2011, **3**, 154–9.

33. M. Glei and W. Schlörmann, *Methods Mol. Biol.*, 2014, **1094**, 39–48.

34. R. DePalma, C. Liu, F. Barbagini, G. Reekmans, K. Bonroy, W. Laureyn, G. Borghs, and G. Maes, *J. Phys. Chem. C*, 2007, **111**, 12227–12235.

35. A. Fragoso, C. K. O'Sullivan, and L. Civit, *Anal. Biochem.*, 2012, 431, 132–138.

36. C. M. Niemeyer, B. Ceyhan, and D. Blohm, *Bioconjug. Chem.*, **10**, 708–19.

37. Z. Ding, C. J. Long, Y. Hayashi, E. V Bulmus, A. S. Hoffman, and P. S. Stayton, *Bioconjug. Chem.*, **10**, 395–400.

38. Z. Liu, L. Jiang, F. Galli, I. Nederlof, R. C. L. Olsthoorn, G. E. M. Lamers, T. H. Oosterkamp, and J. P. Abrahams, *Adv. Funct. Mater.*, 2010, **20**, 2857–2865.

39. M. L. S. Mello and B. C. Vidal, *PLoS One*, 2012, **7**, e43169.

40. M. Banyay, M. Sarkar, and A. Gräslund, *Biophys. Chem.*, 2003, **104**, 477–88.

41. I. Dumazet-Bonnamour and P. Le Perchec, *Colloids Surfaces A Physicochem. Eng. Asp.*, 2000, **173**, 61–71.

42. G. D. Mendenhall, Y. Geng, and J. Hwang, *J. Colloid Interface Sci.*, 1996, **184**, 519–526.

43. H. R. Marsden, L. Gabrielli, and A. Kros, *Polym. Chem.*, 2010, **1**, 1512.

44. G. M. Whitesides and M. Boncheva, *Proc. Natl. Acad. Sci. U. S. A.*, 2002, **99**, 4769–74.

Figure Captions

Scheme 1: Schematic illustration of the method.

Figure 1: Behaviour of different elution solutions on O_{23} bearing magnetic beads at different temperatures (n=3), **A.** 95 ºC, **B.** 85 ºC, **C.** 75 ºC.

Figure 2: A. FT-IR spectrum of the Naive, DNA bearing and Eluted beads. **B.** Effect of consecutive washes on bead concentration (n=3).

Figure 3: SEM images of the beads after three (**A** and **B**) and nine (**C** and **D**) consecutive washes with B&W. Scale bars are presented below the images.

Figure 4: A. Agarose gel image of PCR products obtained from increased number of thermal cycles. Inset graph shows the surface area of the bands based on pixel intensities **B.** Optimization of the incubation time for O_{23} and O_{94} **C.** Hydrodynamic size of the beads after incubation with 0, 25, 50, 75 µl of PCR products (n=3), inset shows DLS volume intensity of the beads versus size in nm.

Figure 5: A: ssDNA yield at different temperatures. Inset demonstrates agarose gel image of eluted DNA obtained from the heat elution at 75, 85, and 95 ºC, along with 100 bp DNA ladder **B.** Reproducibility of the procedure (n=3).

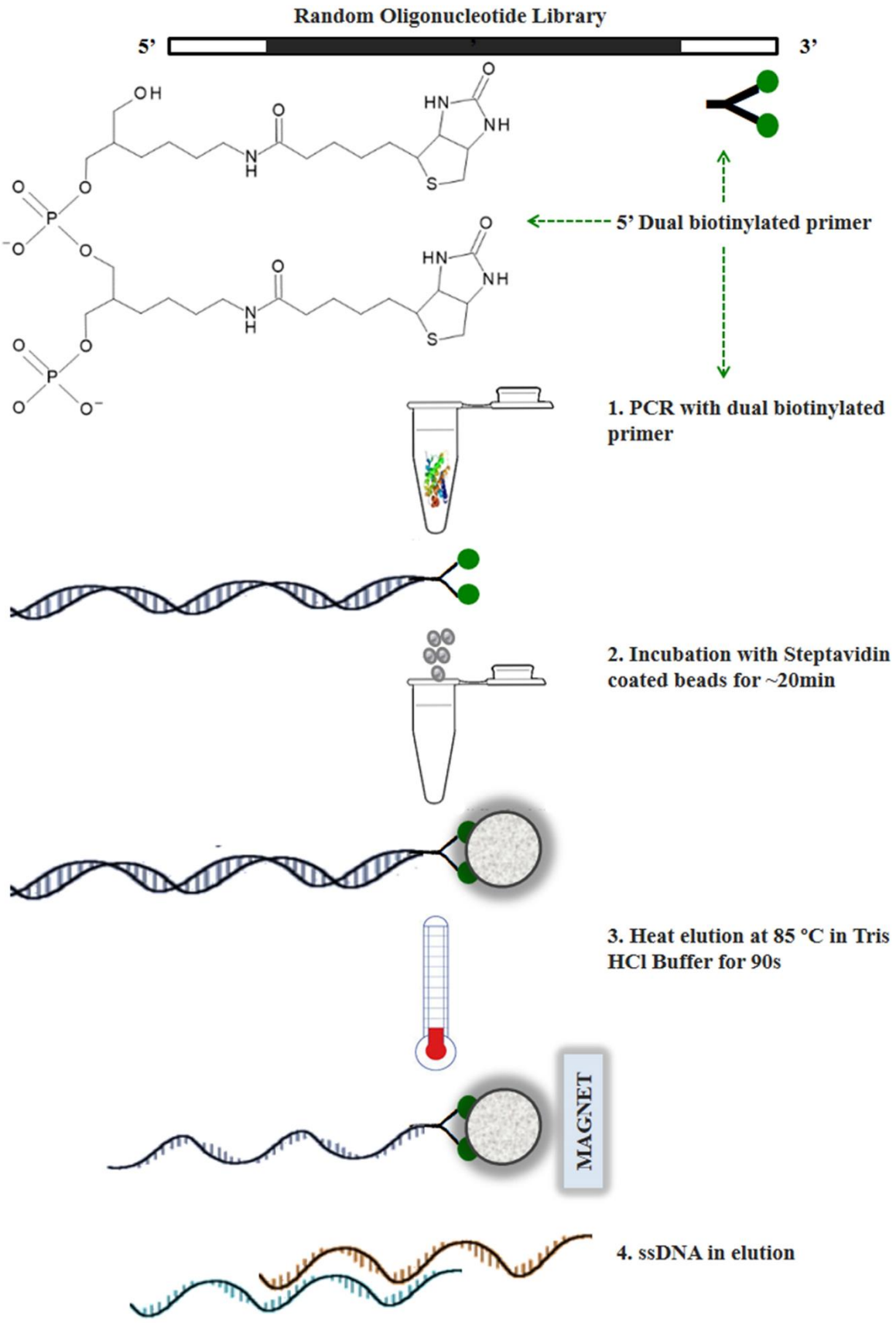

Scheme 1

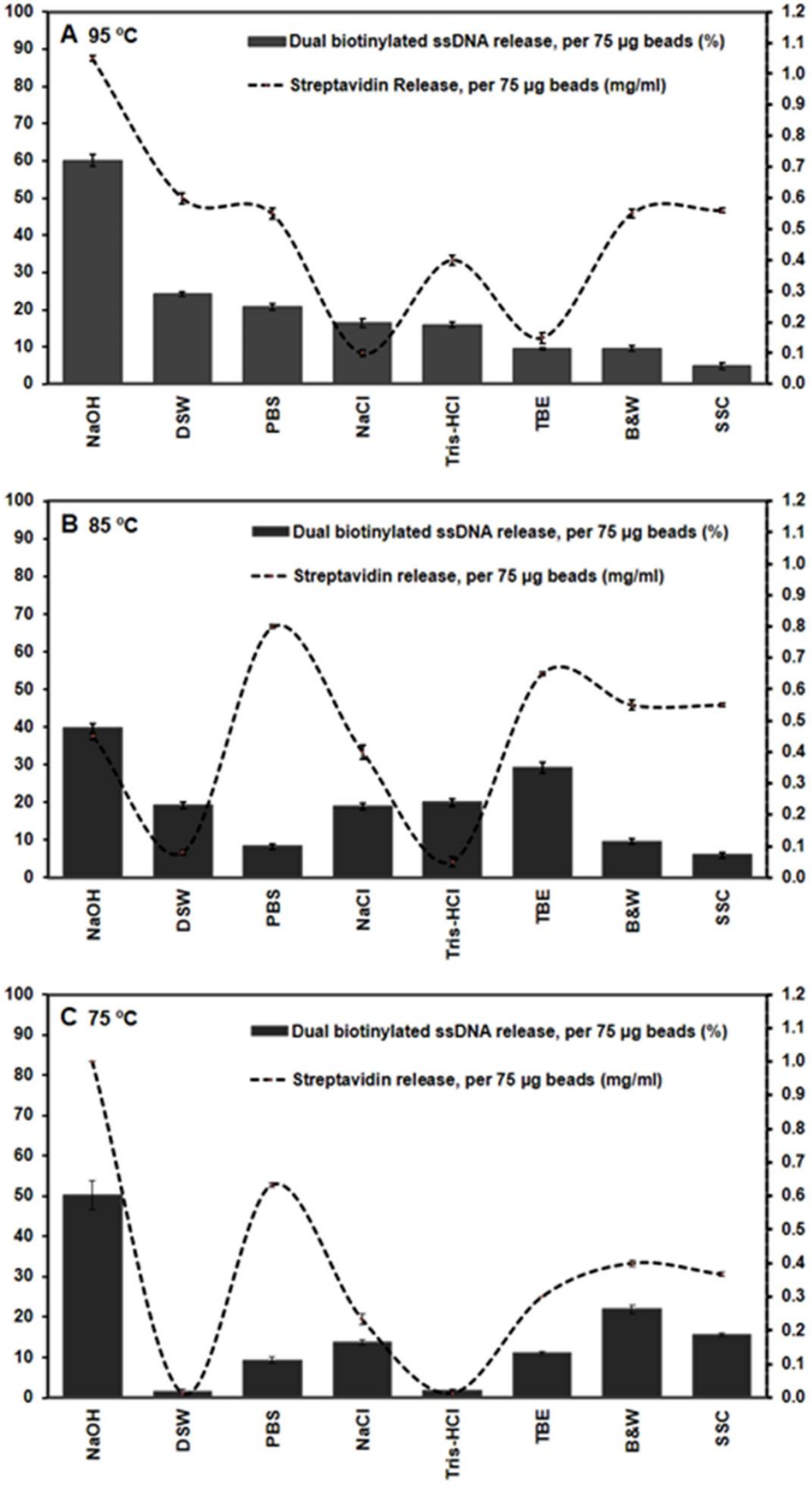

Fig 1

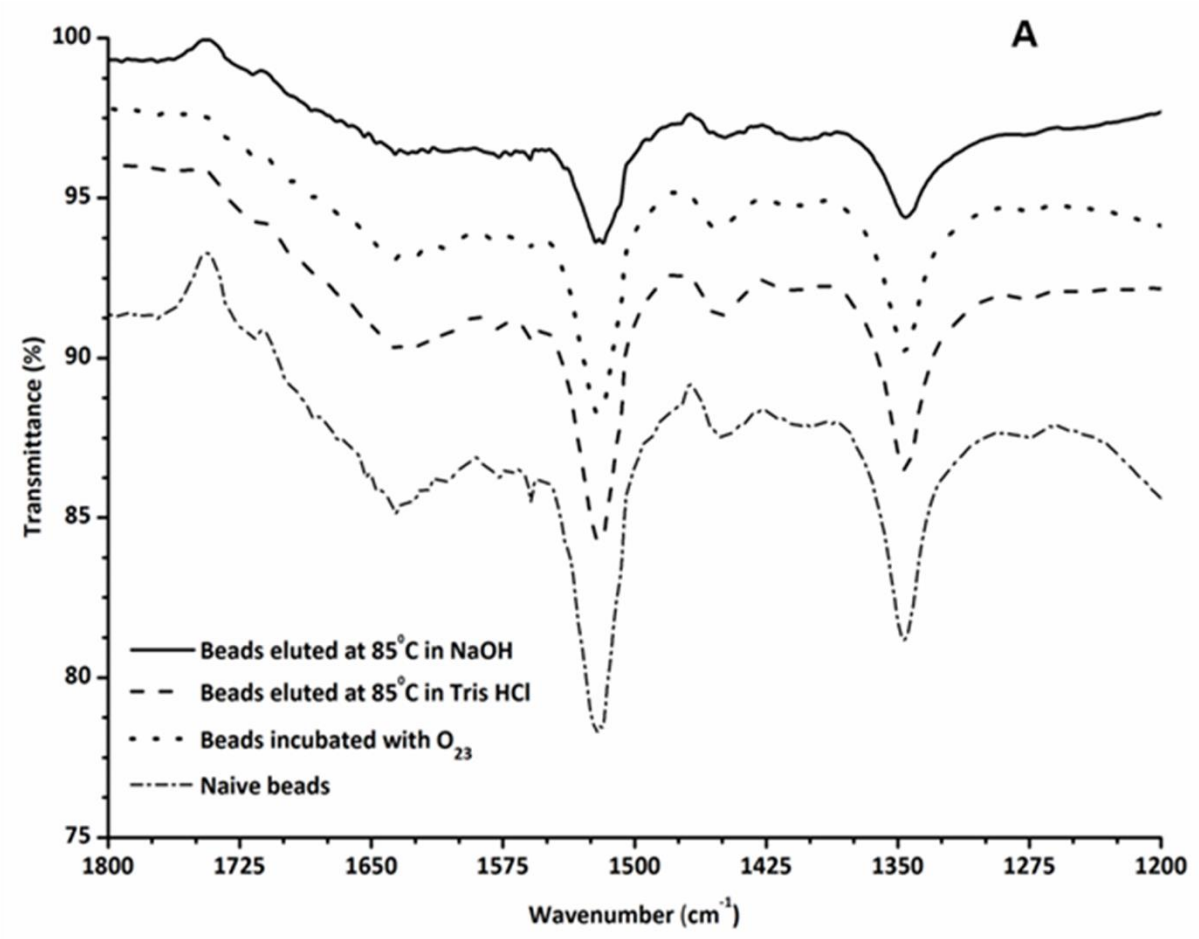

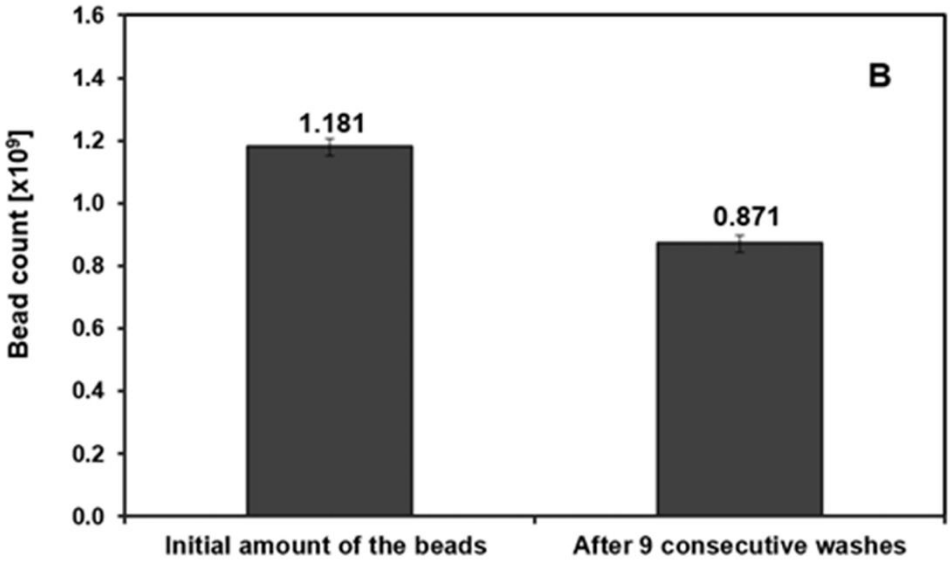

Fig 2

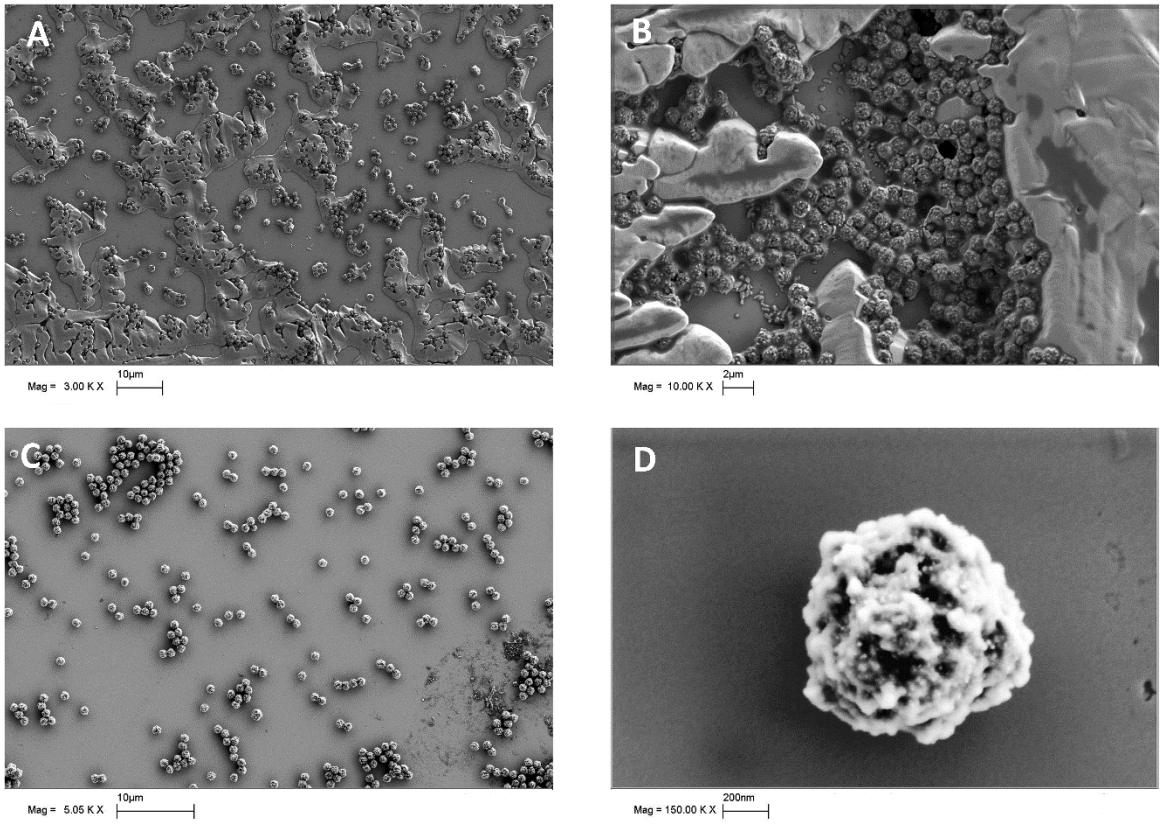

Fig 3

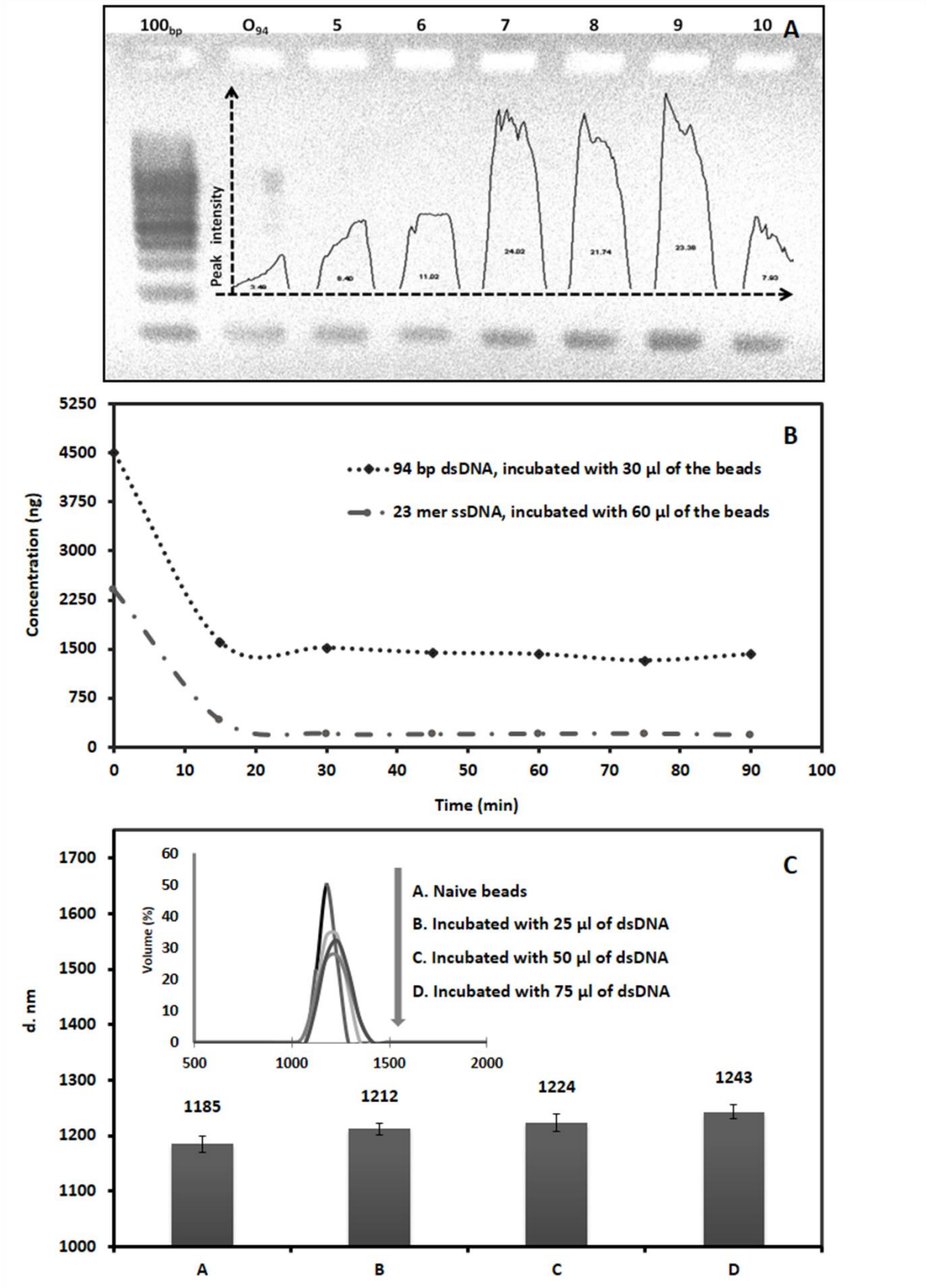

Fig 4

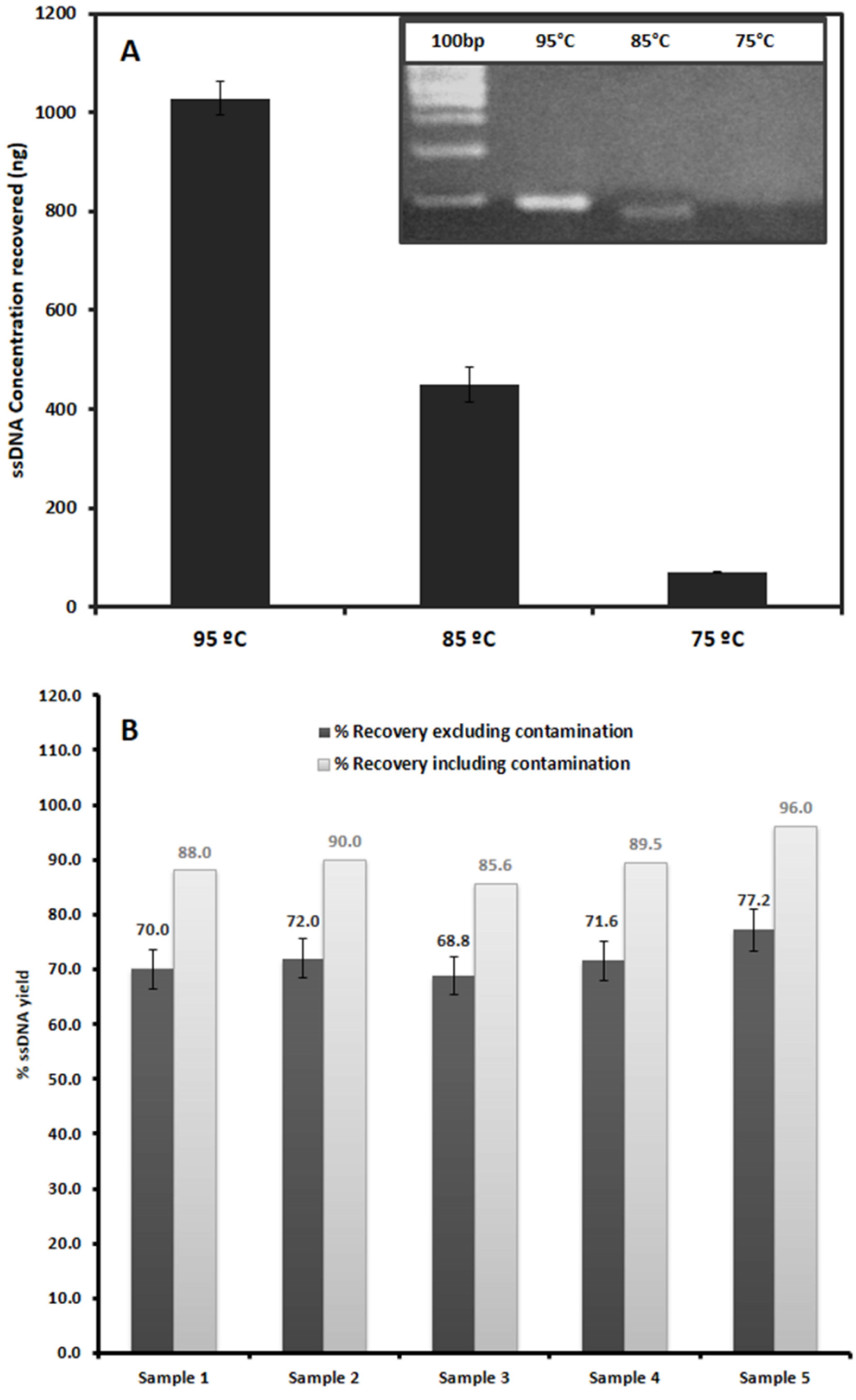

Fig 5